AN UPDATED NUMERICAL MODEL OF THE OHAAKI GEOTHERMAL FIELD

Michael J. O'Sullivan[1], Theo Renaud[1], Michael J. Gravatt[1], Jérémy Riffault[1], Joris Popineau[1], John P. O'Sullivan[1], Nataly Castillo Ruiz[2] and Matthew Sophy[2]

[1]Department of Engineering Science, University of Auckland, 70 Symonds Street, Grafton, Auckland, 1010, New Zealand.

[2]Contact Energy Limited, Wairakei, New Zealand

m.osullivan@auckland.ac.nz

Keywords: *Reservoir modelling, Geothermal, Ohaaki, Broadlands, Leapfrog, conceptual modelling.*

ABSTRACT

The first well was drilled at the Ohaaki geothermal field in 1965 and not long afterwards the University of Auckland began a long collaboration with Contact Energy and its predecessors in modelling the Ohaaki reservoir. The succession of models has been used to inform decision making and aid consent applications. The permeability distribution in the model has evolved over the years to match data, particularly pressure and temperature trends. As the conceptual understanding of the field changes new versions of the model must reflect these changes.

In recent years, we have been developing a modelling framework that can better capture the fault structures, the geology and the geophysics in a numerical reservoir model. This framework is based on mapping a geological model from Leapfrog Geothermal® into an AUTOUGH2 (or Waiwera) computer model. This paper shows how we imposed this framework on to a model of the Ohaaki geothermal field. We have employed techniques to maintain the state of calibration that has been developed over several years in the current numerical model but also allows new rock types to be added easily as our conceptual understanding of the field evolves. In this paper we discuss our techniques for maintaining the match to data while changing the underlying rock distribution. We also demonstrate how we can change the fault structure, geology, alteration model or model grid without too much effort. A new grid structure is used to allow the model to be run in either AUTOUGH2 or Waiwera, in the latter case benefitting from the improved computational speed.

The aim of this work is to increase the transparency of numerical modelling without compromising the complexity that is needed to match the behaviour of the reservoir. Having a numerical model that is closely linked to the languages used by geologists, geophysicists and reservoir engineers allows a complex model to be explained more easily.

1. INTRODUCTION

The Ohaaki geothermal field is in the volcanic and sedimentary accumulation basin at the eastern margin of the Taupo Volcanic Zone of New Zealand, central North Island (

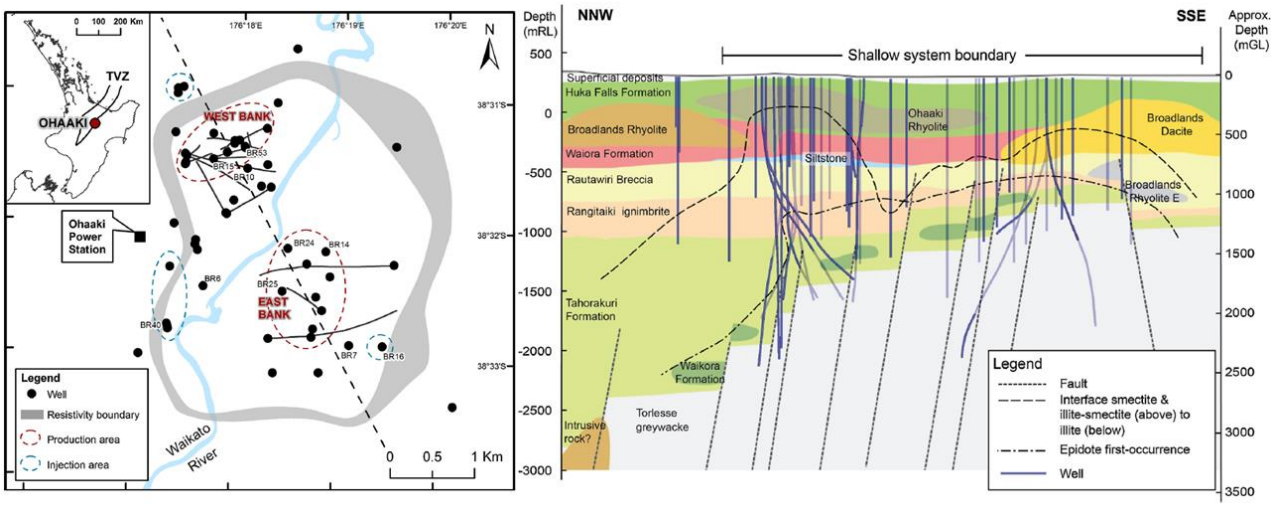

Figure 1, left). High temperatures at ~300°C were encountered at 2400 m in 1968, and the area of the resource was estimated to be 10 km².

The long history of exploration and development of Ohaaki (Lee and Bacon, 2000) started with the drilling of the first well in 1965. Large-scale testing of the production wells was conducted from 1965 to mid-1971 (Clotworthy et al., 1995), but from then until the start of power production in 1989 there was no further production.

The first estimates of potential for power production ranged between 30 and 200 MWe. At the beginning of the 1980s, the production wells supplied enough steam to justify a 116 MWe power station, but with decline rates estimated to be as much as 14% per year, based on data from the production testing period (Lee and Bacon, 2000). By 2000, in the deeper production areas at the time, the

pressure had declined by 15-20 bars, whereas at intermediate depths there was a drawdown of 10 bars, with local variations in response due to reinjection (Lee and Bacon, 2000). Steam zones were first identified in the late 1960s at shallow depths on the West Bank, and later developed on the East Bank. Outflows of mass at 10 kg/s and heat at ~75 MWth were estimated for the boiling Ohaaki Pool or Ngawha.

More than 70 wells have been drilled at Ohaaki. Between 1965 and 1988 depths in the range 1100-1400 m were targeted, but after 1995 some deeper wells (up to 3000 m) were drilled (Rae et al., 2007; Carey et al., 2013; Mroczek et al., 2016). Approximately 90 % of the wells are productive, with feedzones mostly located below the Huka falls formation and extending all the way down to the greywacke basement, typically encountering the 260°C isotherm at an elevation of around -700 mRL. Also, the base of the Ohaaki rhyolite has shown evidence of permeability (+50 to -150 mRL).

The deep wells drilled after 1995 were all on the West Bank, increasing production from there and decreasing production from the East Bank.

The conceptual model of the reservoir has improved over the years thanks to the integration of more information like magneto-tellurics data (MT) and deeper drilling data. Also, tracer tests have highlighted subsurface interconnections with surrounding aquifers and identified isolated zones in the reservoir. The West Bank deep reservoir zone has shown a large pressure decline with some pressure recovery between 2001 and 2010. Nevertheless, the deep reservoir is thought to be connected to the intermediate reservoir, but the pressure data suggest that there is a low permeability zone between the deep wells and intermediate level wells.

The East Bank pressure appears to be slightly higher than that in the West Bank, suggesting the existence of a separate deep upflow in the West (Mroczek et al., 2016).

Figure 1 (right) shows a cross section from a three dimensional (3D) conceptual model discussed by Mroczek et al. (2016). The geothermal system appears to overlay the greywacke basement rocks which dip to the northwest with a horst structure in the south east. The Rangitaiki ignimbrite which erupted 350,000 years ago is a marker for the Whakamaru group. The Huka falls group represent impermeable fine-grained sediments and the Waiora and Rautawiri formations are shallow tuffs. A thick Ohaaki rhyolite dome is located on the West Bank. This dome is highly faulted and permeable and allows the geothermal fluid to rise up through it.

The location of deep sources at Ohaaki is discussed in Mroczek et al. (2016). They suggest the main contribution is from the north west, following the basement structure and controlled by faults.

Hydrothermal alteration has been observed throughout the reservoir, with smectite at shallow depths, transitioning to illite at depths of around 400-600 m. The alterations form a low permeability, clay cap for the system.

During the production history, subsidence at rates of up to 100 mm/yr has been observed around the steamfield (e.g., Allis and Zhan, 2000).

The numerical model of the Ohaaki geothermal field discussed here is an experimental research model and is complementary to current operational model used by Contact Energy Limited. It includes the clay cap and an improved representation of the 3D fault network. The leapfrog-based model is used to investigate the natural state and the production history of the system using the new simulator Waiwera.

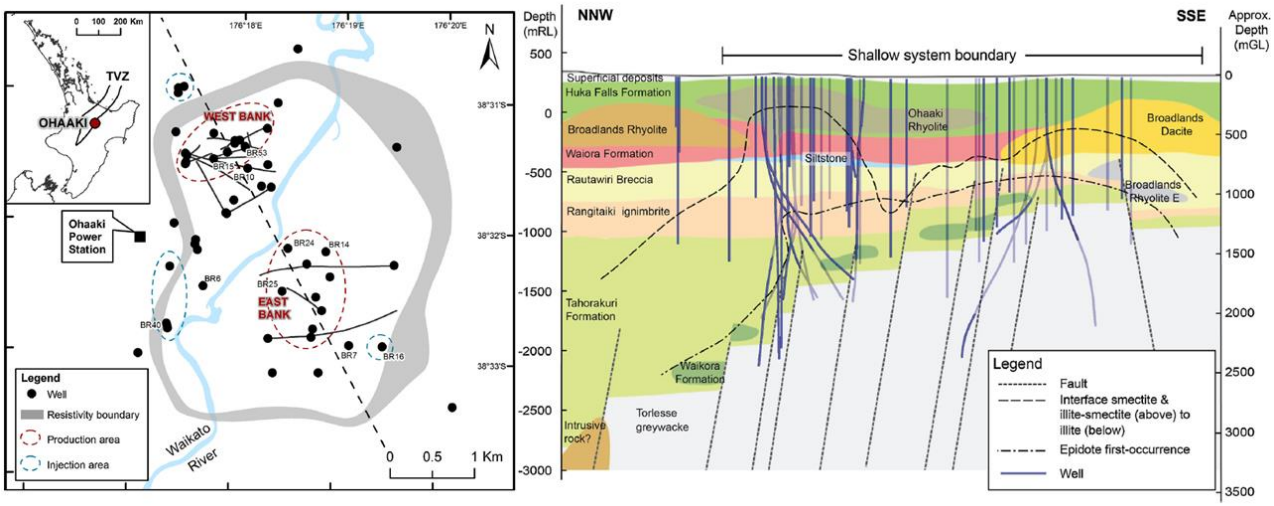

Figure 1: Left, Location of the Ohaaki Geothermal Field. Right, Cross section of a 3D model from Mroczek et al. (2016).

Proceedings 43rd New Zealand Geothermal Workshop
23-25 November 2021
Wellington, New Zealand
ISSN 2703-4275

2. MODEL SETUP

2.2. Geological model

An updated version of the geological model has been built using Leapfrog Geothermal® by GNS Science, notably mapping twelve faults in the area. Figure 2 shows the fault network, including the three regional faults, Aratiata, Reporoa Caldera, Kaingaroa, and nine northeast striking faults. Some faults dip to the South or North by a few degrees. Several intersections between faults are located within the West Bank.

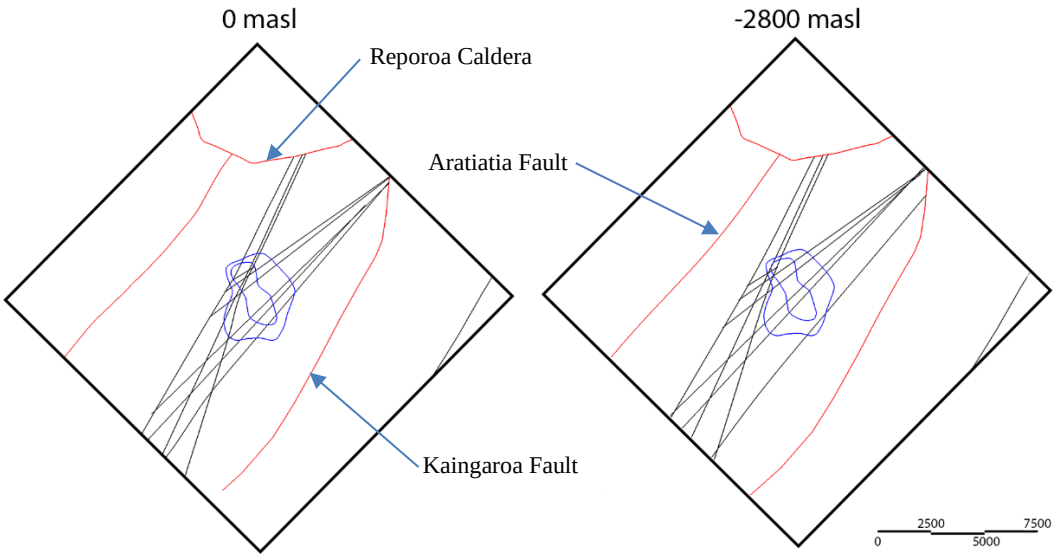

Figure 2: Updated fault network in the model displayed in Leapfrog.

The definition of an alteration model allows more heterogeneity in the permeability structures of the numerical model and this should allow better calibration of the shallow temperatures. The alteration zone is represented by new rock-types in the numerical model. As well as alterations, four other data sources define the alteration zone or clay cap shown in Figure 3: magneto-telluric data (MT), downhole temperature data (contoured into surfaces in Leapfrog Geothermal®), the DC resistivity boundaries and feed zone information for the wells.

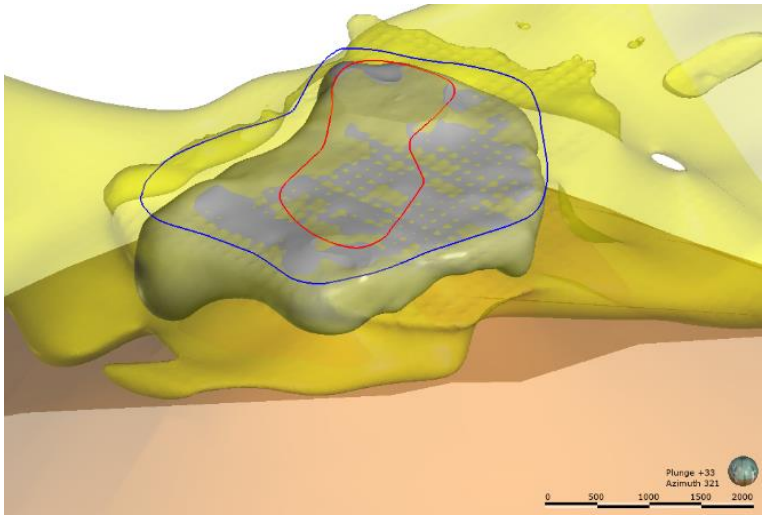

Figure 3: Clay cap (grey) showing the 9 ohm-m MT contour (yellow), the DC resistivity boundary (blue and red) and the 200°C temperature contour (orange)).

2.3 Grid

Various options were considered for the grid for new model but finally a regular rectangular grid was chosen. The main reasons for the choice were that, first, it enables high resolution representation of the faults and, secondly it can use the same small blocks in the inner reservoir as in the current operational model (see Fig. 4)

Hence a new model for Waiwera, based on a regular rectangular grid, was created by mapping over the updated Leapfrog geological model. Figure 4 shows the current 38,582 grid and with the new 69,095 model superimposed. As mentioned above, it allows a higher resolution for the faults while matching the refinement of the old grid in the central area. There are more blocks in the updated grid but using the simulator Waiwera enables faster computation (see Section 4).

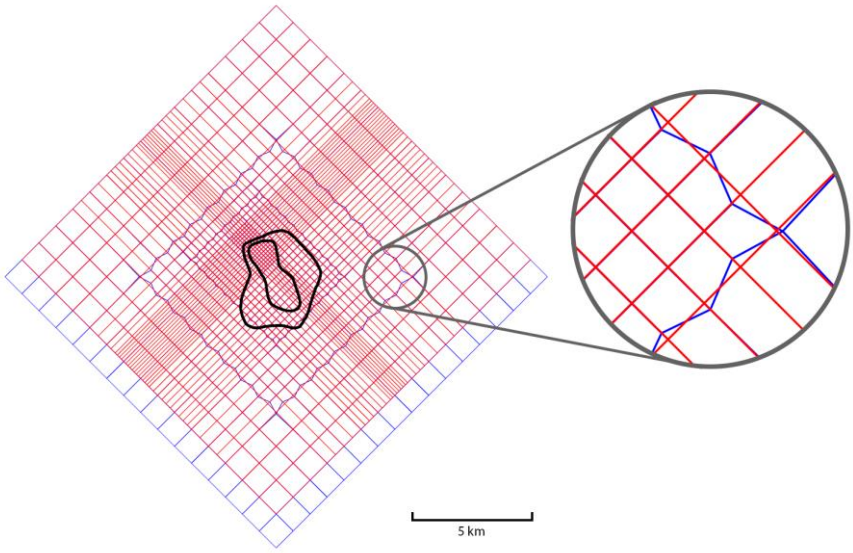

Figure 4: Differences between the old grid (blue) and new rectangular grid (red). The DC resistivity boundary is shown.

2.4 Permeability distribution

A naming convention for the rock-types in the numerical model was set up to allow heterogeneity in the assignment of permeability. The rock-type name uses a code containing letters and digits, which identifies the following:

- Basic formation encountered,
- Intersections with the faults or the clay cap,
- If a sub-rock-types within faults or formations should be used.

In the old 38582 model, the permeability distribution was based on older geological models and the structural model has only been partly implemented. For example, a permeable, vertical pathway connecting the Ohaaki Pool area to the deep reservoir was implemented. Because of observed cooling trends this high permeable vertical connection is thought to exist around well BR09 and extend further down towards wells BR59, BR60, BR61 and other wells (Brockbank and Bixley, 2011). However, the complete structural model was not implemented in the 38582 model and one of the main aims in setting up the new 69095 model was to include the full structural model.

Cutting over from the 38582 model to the 69095 model was a challenging task for the following reasons:

- We wish to have a permeability distribution that fully reflects all aspects of the Leapfrog model (formations, structures, alterations).
- The 38582 model is quite well calibrated and therefore we wish to maintain a similar permeability distribution in the first version of the 69095 model.
- The system for setting up the rock-type distribution needs to be easy to implement and mesh independent so that future changes to the Leapfrog model will be easy to incorporate and mesh refinement can also be easily implemented.

Some changes to the locations of faults and minor changes to the locations of formations were made in the 69095 model. For example, Figure 5 shows the differences in the rock-type distribution in the deepest layer between the two numerical models.

The following steps were followed in setting up the rock-type distribution in the 69095 model:

(a) First rock-types were set up taking account of the formations, structures and alteration. For example, S0000 is the basic alluvium formation, S00A0 is an altered version of alluvium in the clay cap, SA000 corresponds to where Fault A intersects the alluvium, SAC00 corresponds to where Fault A and Fault C intersect the alluvium, etc.
(b) To allow direct transfer of permeabilities from the 38582 model to the 69095 model multiple versions of some rock-types were introduced. For example, as well as the rock-types listed in (a) we added S0002, S00A1, SA002, SAC02.

Because of the more accurate representation of faults in the 69095 model, the transfer of some permeabilities from the 38582 model resulted in a few unphysical results, e.g., a low permeability in a faulted block or a high permeability in a block in an un-faulted base formation. These potentially problematic rock-types were left unchanged but in re-calibration of the 69095 model it is expected that they will be changed.

Proceedings 43rd New Zealand Geothermal Workshop
23-25 November 2021
Wellington, New Zealand
ISSN 2703-4275

In some cases, the location of the formation boundaries was changed. For example, the elevation of the top of the basement was raised in the new model, replacing the Tahorakuri formation in several blocks. To accommodate this change, a second basement rock-type was introduced with the same properties as the Tahorakuri formation in the 38582 model.

In the early stages of the recalibration of the 69095 model the parameters of various rock-types were adjusted to give better representation of the faults.

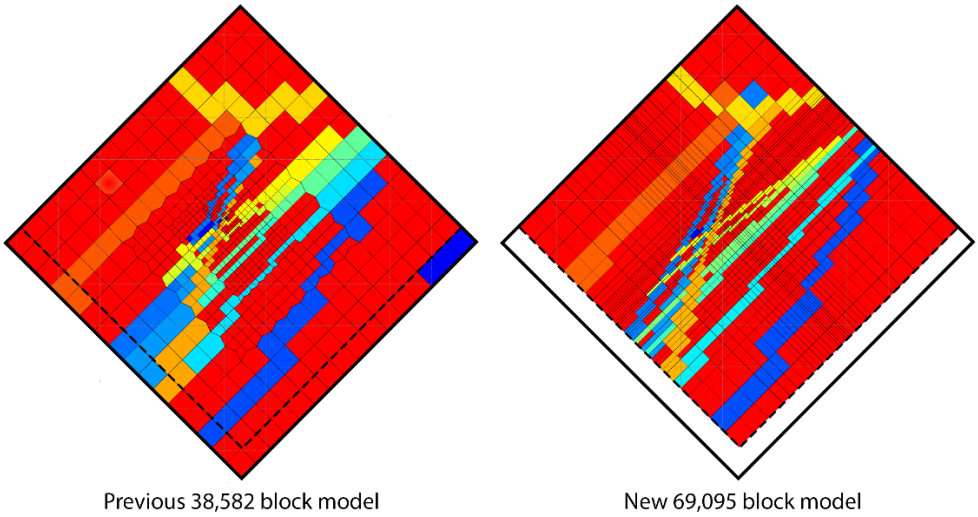

Figure 5: Rock-type distribution differences between the two grids (old and new).

In the updated model, the faults extend from the bottom layer (-3575 m) to the topographic surface, while in the old model they stop at various elevations (from -1825 m to -350 m). Hence, the updated model has the potential to better represent the flow of hot fluids to the surface or the flow of cold fluids from shallow to deep zones.

It is expected that the very first permeability distribution mapped on to the 69095 model will not be the same as that used in the 38582 model and re-calibration will be needed. However, by basing the permeability distribution on the updated geological model, the new definition of the faults and the alteration model, it is expected a better computer model will be obtained with a better representation of some areas of the Ohaaki geothermal reservoir.

2.5 Boundary conditions

The natural recharge of heat, mass and CO2 must be specified in the Ohaaki model. Across the whole area, a background conductive heat flow of 70 mW/m² is applied. In addition, deep hot upflows are implemented by the injection of high enthalpy water and CO_2. The CO_2 injected is set at an average mass fraction of 2.5% of the mass upflows. Table 1 presents the input of heat and mass implemented for the natural recharge.

Table 1: Natural recharge used in the Ohaaki model.

Heat input (MW)	15.7
Heat flux (W/m²)	0.07
Water input (kg/s)	141.2
CO2 input (kg/s)	3.53
CO2 input (%)	2.5
Average enthalpy (kJ/kg)	1.42e3

From the 38582 model, the upflows were mapped over to the 69095 model at the same locations. Figure 6 shows the deep mass input distribution for the two models, all implemented in faulted blocks.

No-flow boundary conditions are set laterally which is a reasonable approximation as pressures near the boundaries remain almost unchanged.

At the top boundary, atmospheric conditions are applied, with a temperature of 15°C, total pressure of 1 bar and partial pressure of CO_2 of 0.9962 bar. The Waikato River and Waiotapu Stream are represented in the model with “wet” atmospheric blocks at the top of the relevant columns. These correspond to a temperature of 10°C and a hydrostatic pressure of a 10 m water column. In dry land blocks, cold water is injected at a rate of 10% of the annual average rainfall of 1325 mm/year.

ISSN 2703-4275

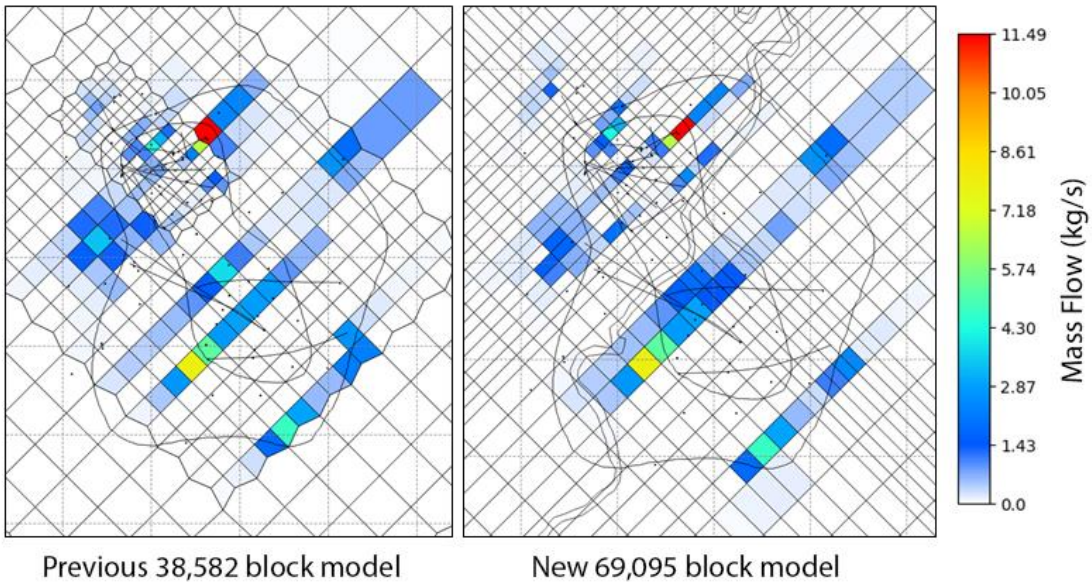

Figure 6: Mass upflow at the base of the model, showing the differences between the previous 38582 model and the new 69095 model.

3. RESULTS

3.2 Natural state

Calibration of the 69095 model has commenced and preliminary results are shown below. For the various stages of calibration, we calculate measures of the fit of the model results to the data. For example, we calculate errors between all the temperature data and the corresponding model result and then produce histograms of the distribution of errors. The plots for the 38582 model and the 69095 model are shown as Figure 7 and Figure 8, respectively. The plots show that the match achieved with the 69095 model is not yet as good as that achieved with the 38582 model, however we expect it will improve significantly with more effort spent on re-calibration. Similar comments apply to the state of calibration of the production history model.

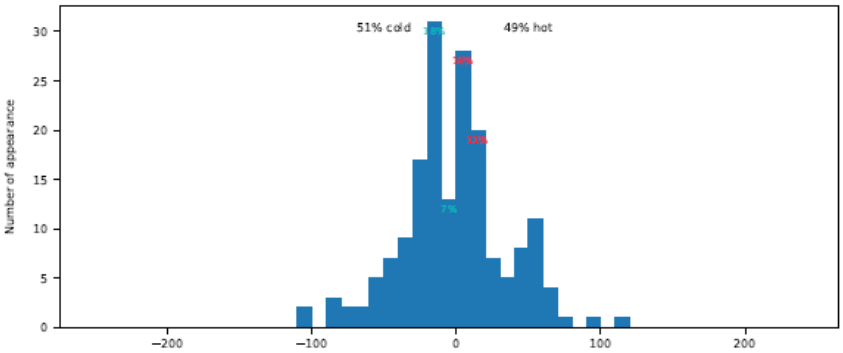

Figure 7: Histogram of temperature errors for model 38582

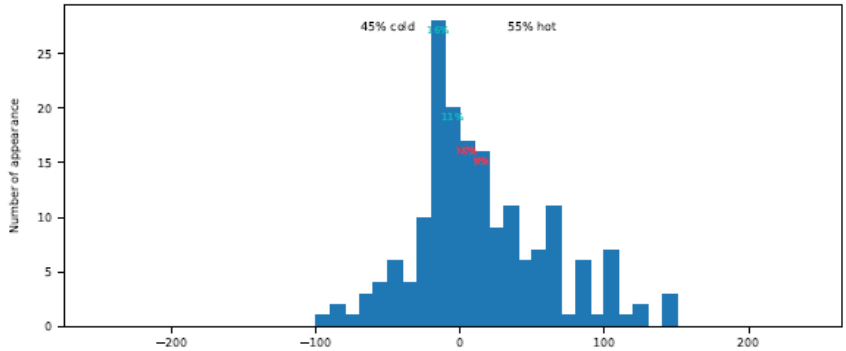

Figure 8: Histogram of temperature errors for model 69095

Proceedings 43rd New Zealand Geothermal Workshop
23-25 November 2021
Wellington, New Zealand
ISSN 2703-4275

Figure 9 displays the NW-SE cross section of the natural state temperature. Overall temperature profiles on the West Bank are well matched, as shown in Figure 10. Some of the details require improvement, e.g., the low temperature zone at -100 mRL in well BR17. The model is too hot for BR33. In the East Bank, a good match to the natural state temperature profiles is obtained (see Fig. 11). Again, there is potential for improvement, e.g., at present there is too much cold inflow in BR24 between -750 and -1000 mRL.

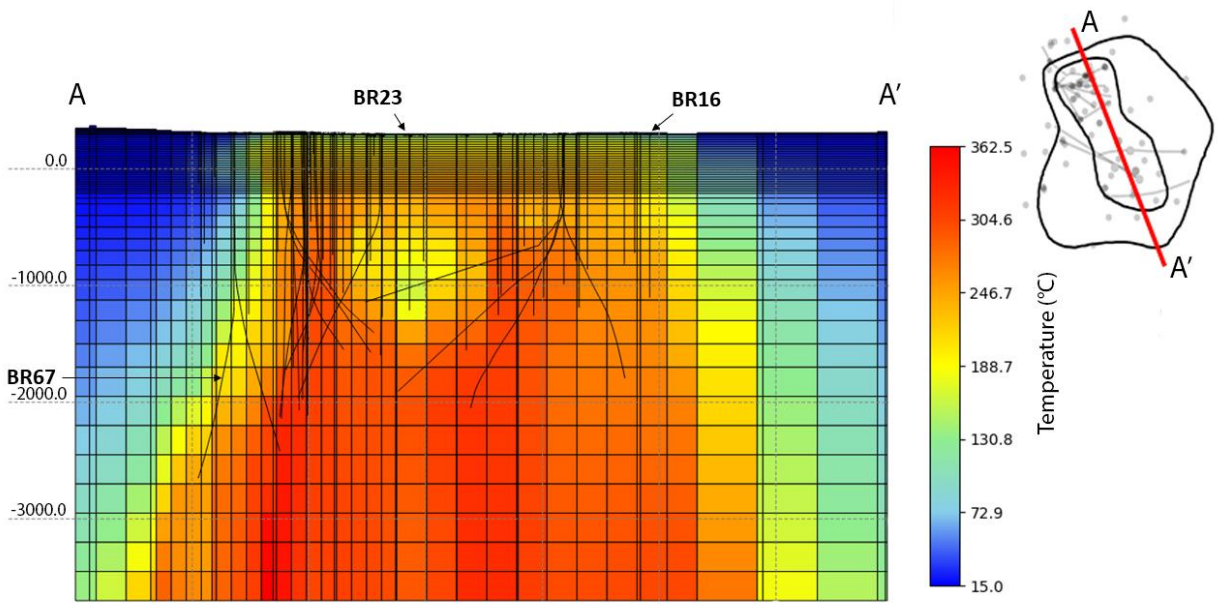

Figure 9: Natural state temperature distribution on the model along a NW-SE slice as indicated in the diagram in the top left.

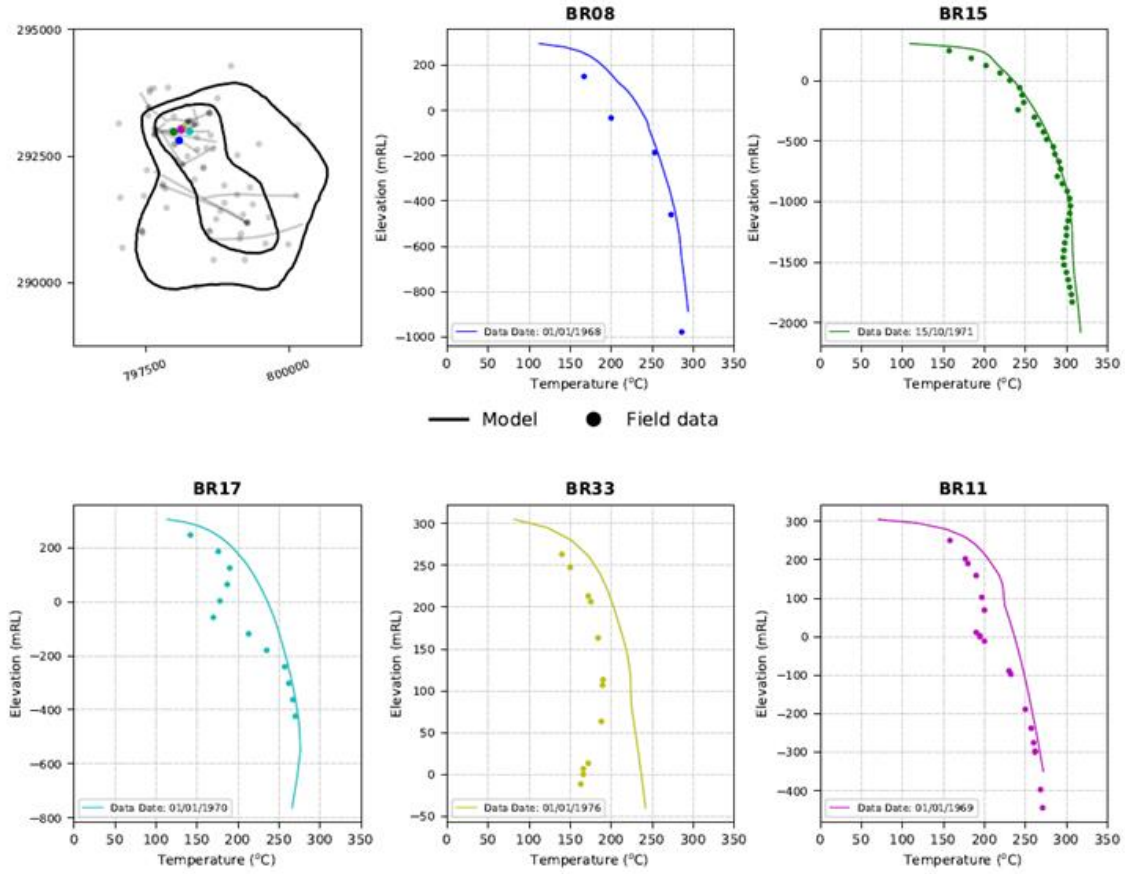

Figure 10: Natural state comparison between the model and downhole temperature data on the West Bank.

Proceedings 43rd New Zealand Geothermal Workshop
23-25 November 2021
Wellington, New Zealand
ISSN 2703-4275

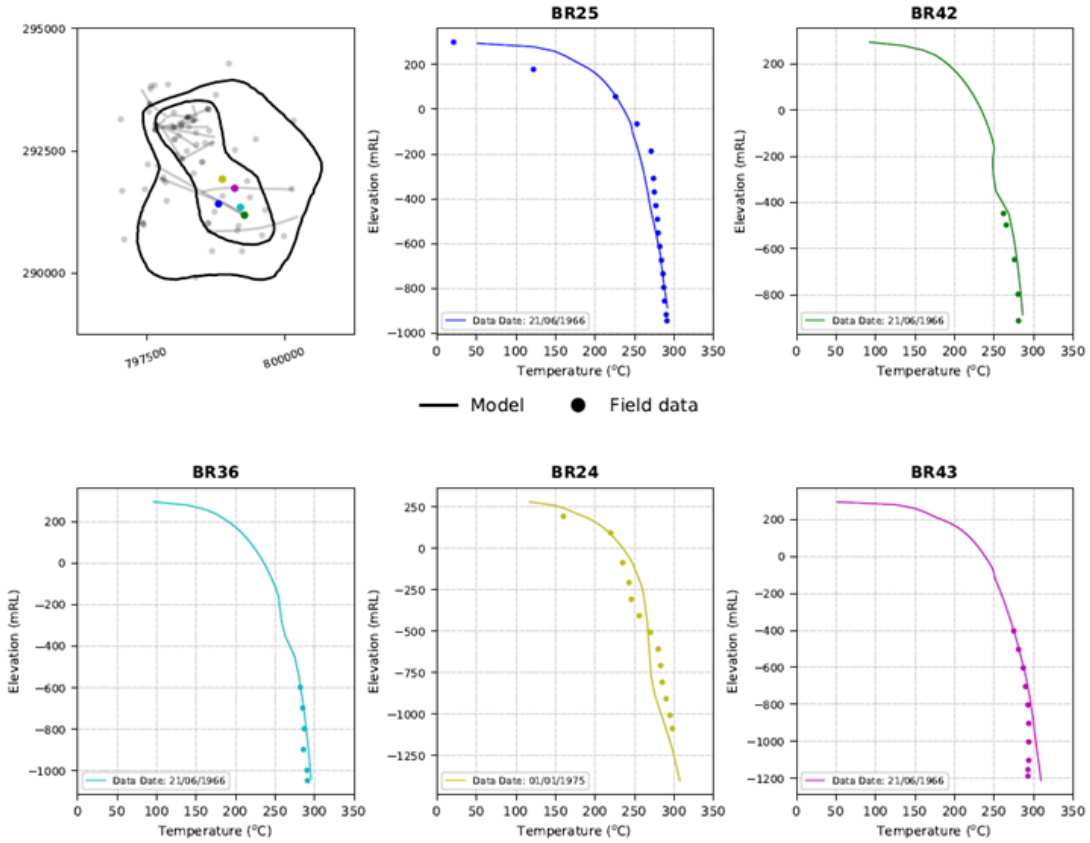

Figure 11: Natural state comparison between the model and downhole temperature data on the East Bank.

3.3 Production history match

A good match to all the production data is more difficult to achieve. Figure shows plots of temperature, pressure and CO_2 versus time in well BR9 in the West Bank; and the two wells BR25 and BR 36 in the East Bank. The plots highlight the difficulty in matching the decreasing trend of the temperatures in these wells. A decrease in temperature of 50°C has been observed during production, but is not yet obtained in the model. The match to the pressure data is good for BR9 and BR25 but more calibration is required to better match the 30 bar pressure drop in the well BR36 in the early 1990s. The modelling of the CO_2 discharge partly captures the observed data but shows some inconsistency in matching the peaks in the data.

ISSN 2703-4275

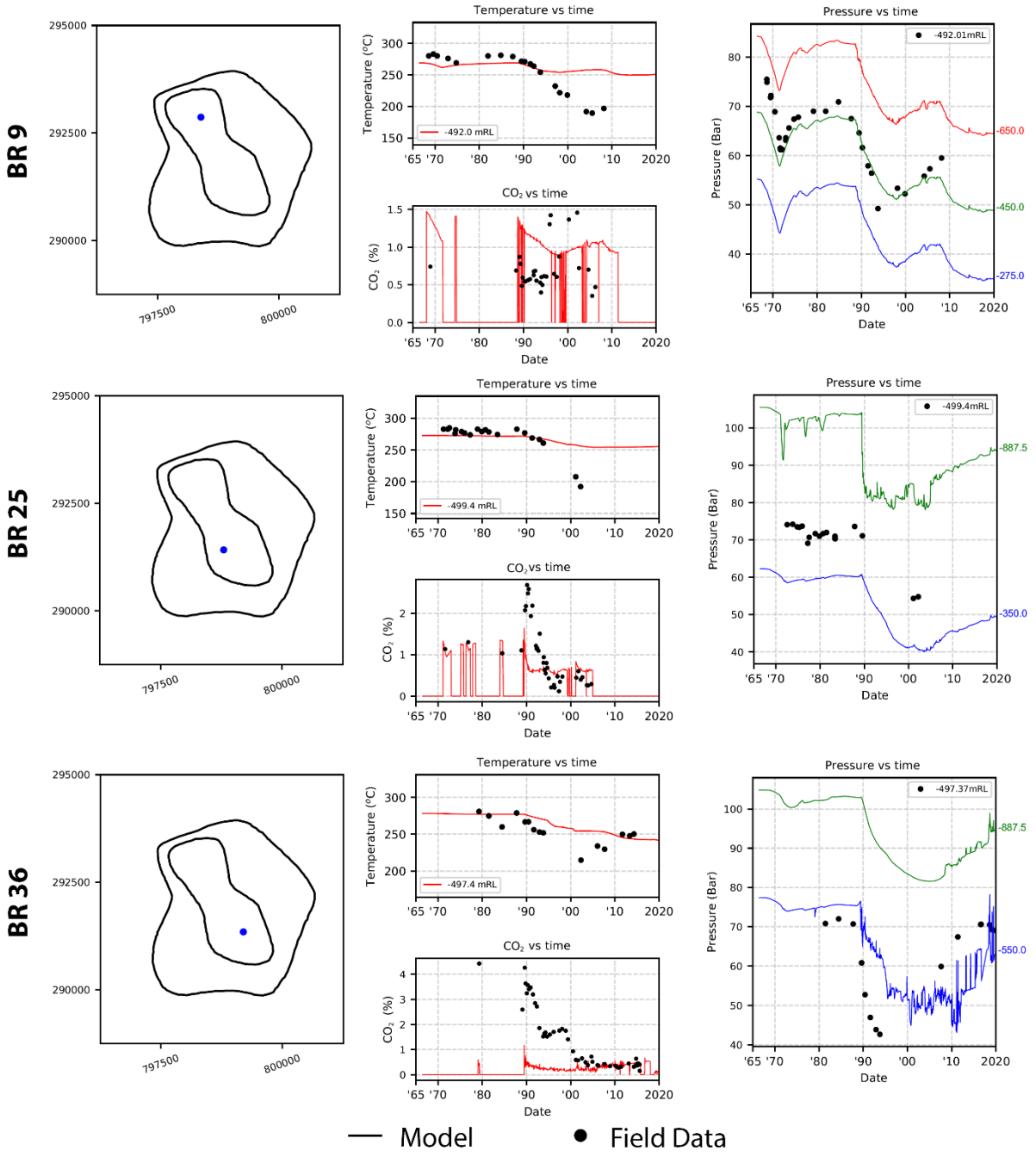

Figure 7: Production history match to data for BR9, BR25 and BR36 for temperature, pressure and CO_2 data.

4. DISCUSSION

The updated 69095 model can be run in either AUTOUGH2 (Yeh et al., 2012) or the highly parallelized simulator Waiwera (Croucher et al., 2020). The significant decrease in the computational time shown in Table 2, allows a speed-up of the calibration process currently being undertaken. Hence, calibration uses both simulators, using in-house python scripts to convert the results obtained into initial conditions for one another. Using the same version with both simulators allows us to maintain an accurate AUTOUGH2 model with mature post processing visualization tools such as TIM (Yeh et al. 2013). At present it is necessary to continue using AUTOUGH2 as it offers many more options for specifying future scenario. Work on Waiwera is continuing on the implementation of more options for specifying wells, e.g., to allow automatic addition of make-up wells to meet a target total steam flow.

The implementation of the equation of state for H_2O-CO_2 mixtures is slightly different between AUTOUGH2 and Waiwera but this difference does not appear to have a significant effect on the model results. Table 2 displays the computational time for both models, using AUTOUGH2 or the parallel simulator Waiwera. It shows Waiwera can offer a speed-up by a factor of 20-40 times compared to AUTOUGH2.With faster calibration, more time can be allocated to model improvement.

Table 2: Time comparison for the Natural State and the Production history simulations between AUTOUGH2 and Waiwera

Model	Natural State	Production History
AUT2 - 38,582	195 mins* (3.2 h)	385 mins (6.4 h)
AUT2 - 69,095	2456 min (~40 h)**, 79 mins* (1.3 h)	1030 mins (17.15 h)
Waiwera - 69,095 (40 Cores)	80 min (1.3 h) **, 27 mins* (0.45h)	48 min (0.8 h)

* Run times are indicative only, depends on how much the parameters are changed from the previous calibration.

** Run from a warm 30°C/km thermal gradient and hydrostatic pressure.

5. CONCLUSIONS

The new 69095 model is fully integrated with a Leapfrog Geothermal® representation of the conceptual model including the updated 3D distribution of the geological formations and structures. In addition, an alteration model, defining a clay cap zone with new rock-types for the reservoir model is implemented. The scripts used to generate the AUTOUGH2 (or Waiwera) model are sufficiently general so that changes to the conceptual model and/or mesh refinement could easily be accommodated. The permeability distribution from the old 38582 model was used as the starting point for assigning rock-type parameters in the new model and after some re-calibration a reasonable match to natural state and production history was achieved. It is expected that with some further calibration the 69095 model will better match all the field data while at the same time honouring the conceptual model.

By running AUTOUGH2 and Waiwera versions of the model in parallel we are able to take advantage of both the superior computational performance of Waiwera and the generality of well types available in AUTOUGH2.

ACKNOWLEDGEMENTS

We thank Contact Energy Limited for permission to publish this paper.

REFERENCES

Allis, R.A. and Zhan, X.: Predicting subsidence at Wairakei and Ohaaki geothermal fields, New Zealand. Geothermic, 29, 479-497 (2000)

Brockbank, K.M. and Bixley, P.F.: The Ohaaki Deep Reservoir. *Proc. 33rd New Zealand Geothermal Workshop*, Auckland, New Zealand. (2011).

Carey, B., Alcaraz, S., Soengkono, S., Mroczek, E., Bixley, P., Rae, A., Lewis, B, Reeves, R. and Bromley, C.: *Ohaaki Geothermal Power Plant. Project Reference Report: Geoscientific and Reservoir Engineering Review*. GNS Science Consultancy Report 2011/273, 236p., (also Appendix C to Part B, the Assessment of Environmental Effects Report, submitted by Contact Energy to the Waikato Regional Council in support of an application for Resource Consents for the Ohaaki Geothermal Power Plant). (2013).

Clotworthy, A., Lovelock, B., Carey, B.: Operational History of the Ohaaki Geothermal Field, New Zealand, *Proc. World Geothermal Congress 1995*, Florence, Italy. (1995).

Croucher, A., O'Sullivan, M., O'Sullivan, J., Yeh, A., Burnell, J., Kissling, W.: Waiwera: A parallel open-source geothermal flow simulator. *Computers and Geosciences*, *141* (2020).

Lee, S., Bacon, L.: Operational history of the Ohaaki geothermal field, New Zealand. *Proc World Geothermal Congress 2000*, Kyushu-Tohoku, Japan. (2000).

Mroczek, E.Z., Milicich, C.D., Bixley, P.F, Sepulveda, F.,Bertrand, E.A., Soengkono.,S, Rae, A.J.: Ohaaki geothermal system: Refinement of a conceptual reservoir model. *Geothermics*, 59, pp. 311-324. (2016).

O'Sullivan, M., Gravatt, M., Popineau, J., O'Sullivan, J., Mannington, W., McDowell, J.: Carbon Dioxide emissions from geothermal power plants. Renewable Energy, 175, pp. 990-1000 (2021).

Rae, A.J., Rosenberg, M.D., G. Bignall, G., Kilgour, G.N. and Milicich, S.: Geological Results of Production Well Drilling in the Western Steamfield, Ohaaki Geothermal System: 2005-2007. *Proc. 29th New Zealand Geothermal Workshop*, Auckland, New Zealand. (2007).

Yeh, A., Croucher, A.E., O'Sullivan, M.J.: Recent developments in the AUTOUGH2 simulator. *Proc. TOUGH Symposium 2012*, Berkeley, California, USA (2012).

Yeh, A., Croucher, A.E., O'Sullivan, M.J.: TIM – Yet another graphical tool for TOUGH2. *Proc. 35th New Zealand Geothermal Workshop*, Auckland, New Zealand. (2013).

ISSN 2703-4275